THE JOURNAL OF PHYSICAL CHEMISTRY B

pubs.acs.org/JPCB Article

Crystal Nucleation Kinetics in Supercooled Germanium: MD Simulations versus Experimental Data

Azat O. Tipeev,* Edgar D. Zanotto, and José P. Rino

Cite This: J. Phys. Chem. B 2020, 124, 7979–7988 Read Online

ACCESS | Metrics & More | Article Recommendations

ABSTRACT: The validity of the classical nucleation theory (CNT), the most important tool to describe and predict nucleation kinetics in supercooled liquids, has been at stake for almost a century. Here, we carried out comprehensive molecular dynamics simulations of the nucleation kinetics of a fast quenched supercooled germanium using the Stillinger−Weber potential at six temperatures, covering a supercooling range of $T/T_m = 0.70-0.86$, where T_m is the equilibrium melting temperature. We used the seeding method to determine the number of particles in the critical crystal nuclei at each supercooling, which yielded $n_* = 150-1300$ atoms. The transport coefficient at the liquid/nucleus interface and the melting point were also obtained from the simulations. Using the parameters resulting directly from the simulations, the CNT embraces the experimental nucleation rates, $J(T)$, with the following fitted (average) values of the nucleus/liquid interfacial free energy: $\gamma = 0.244$ and 0.201 J/m^2, for the experimental and calculated values of thermodynamic driving force, $\Delta\mu(T)$, respectively, which are close to the value obtained from $n_*(T)$. Without using any fit parameter, the calculated nucleation rates for the experimental and calculated values of $\Delta\mu(T)$ embrace the experimental $J(T)$ curve. Therefore, this finding favors the validity of the CNT.

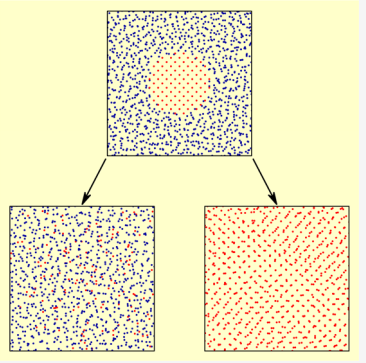

1. INTRODUCTION

Supercooled liquids (SCLs)—liquids that have been cooled below their equilibrium melting point—start to decay with the advent of heterophase fluctuations that eventually lead to the birth of the first critical crystal nucleus. Then, crystallization takes over because crystal growth spontaneously proceeds. The formation of critical nuclei is of great interest because it is not only related to the stability of the parent SCL but also to the relevant technological task of producing new glassy or crystalline materials.[1] The kinetics of homogeneous crystal nucleation in SCLs has frequently been (semiquantitatively) described by the classical nucleation theory (CNT).[2] However, many controversial reports exist regarding its validity.[3] Conflicting views are caused by extreme difficulties to experimentally determine the key quantities, such as the (nanosized) critical nucleus size, the SCL/critical nucleus interfacial free energy, and the diffusion coefficients in SCLs. As a result, using fitted values of γ, the discrepancy between nucleation rates obtained in experiments with glass-forming liquids and calculated by the CNT often ranges from 20 to 55 orders of magnitude.[3]

One of the most appropriate tools to shed light on the crystal nucleation process, at an atomistic level, is computer simulation, in particular molecular dynamics (MD) simulations. MD can obtain essential information on the properties of the crystal nuclei and consequently to test nucleation and crystallization theories. MD simulations have been applied to simulate the crystallization process in numerous model systems, see, for example, ref 4, with different levels of success.

In the current research, we choose germanium as an adequate substance for studying crystallization by MD. Germanium is a material of enormous technological significance,[5] used as semiconductors, which formed the basis for developing transistor technology,[6] with renewed interest triggered by its strong potential for perspective nanotechnologies. The thermodynamic properties of Ge in the stable and metastable regions have been precisely measured,[7−9] which helps in testing theories. However, the most important fact for choosing this particular material is that several interatomic potentials are available, and experimental nucleation rate data have been determined for Ge, which could be used to compare with simulation results.

Supercoolings of germanium droplets achieved by different experimental techniques have been reported in several studies,[1,9−20] down to $T = 0.65 \cdot T_m$, where $T_m = 1211$ K is the equilibrium melting temperature.[21] Colossal supercooling was achieved by studying the crystallization of amorphous

Received: June 16, 2020
Revised: August 15, 2020
Published: August 17, 2020

https://dx.doi.org/10.1021/acs.jpcb.0c05480
J. Phys. Chem. B 2020, 124, 7979−7988

germanium films,[22−24] down to $T = 0.52 \cdot T_m$. The most important aspect for this research work is that the dome-shaped nucleation rate curve, $J(T)$, was experimentally determined by different authors.[1,15,22−24] The glass-transition temperature, $T_g = 489$ K $= 0.40 \cdot T_m$,[25] corresponding to a critical cooling rate of $5 \cdot 10^5$ K/s, was determined from experimental data. In ref 26, the crystallization of germanium liquid droplets having a diameter range of 0.01−5 μm was studied. For diameters below 0.3 μm, the droplets did not crystallize, instead they vitrified. By fitting the experimental results of spontaneous homogeneous crystallization with CNT calculations, the solid/liquid interfacial free energy, γ—as first realized by Turnbull for metals[27]—was estimated to be $\gamma = 0.246$ J/m^2.[26] It is also notable that the liquid metal-to-semiconductor transition occurs during crystallization of this substance.

However, the maximum value of the experimental nucleation rate of Ge, $J \approx 10^{18}$ s^{-1}·m^{-3},[1,22,23] is much smaller than the typical values of homogeneous nucleation rates that are typically assessed from brute-force MD simulations, $J = 10^{30}$ to 10^{35} s^{-1}·m^{-3}.[4,28] Therefore, to study the crystallization kinetics of supercooled germanium by MD simulations, it is necessary to use additional techniques to accelerate the phase transition.[4] In the current research, we chose the seeding method,[29] in which a crystalline cluster of variable size is artificially inserted into a SCL at the beginning of the simulation. The key feature related to this technique is the following: if the crystalline seed is larger than the critical size nucleus at the certain temperature, it will tend to grow, whereas subcritical nuclei will dissolve in the liquid. This simple approach allows the direct determination of the critical size as a function of temperature. Then, using the CNT formalism, the temperature dependences of both the (orientationally averaged) interfacial free energy of the critical crystal nucleus/SCL and the nucleation rate can be calculated. For this procedure, the effective atomic transport coefficient at the liquid/nucleus interface, the critical nucleus size, and the thermodynamic driving force must be known.

It should be noted that, from an engineering standpoint, the crystal seeding method has been widely used for optimizing and controlling the crystallization process in the preparation of crystalline substances with predetermined properties.[30,31] In MD simulations, the seeding method was first used in 1993 to study the crystal dissolution kinetics of silicon.[32] Since then, the seeding technique has been used to unveil the crystallization mechanism of many different atomic and molecular model systems, see ref 33 and references therein. The influence of the properties and structure of the seed, as well as the effect of the finite-size simulation box on the seeded crystallization were also analyzed.[32−34]

Recently, we successfully applied the seeding approach to study the crystallization kinetics of a Lennard-Jones pair potential liquid, along the zero isobar.[33] We found that the theoretically calculated nucleation rate, obtained from MD seeding data, agrees rather well with its direct MD determination available at one temperature. To the best of our knowledge, comparisons of experimental nucleation rates with the values calculated by the CNT (using parameters obtained from simulations) have been made in only a few studies: for seeded crystallization of water,[35−37] sodium chloride,[38−40] and nickel.[41] We will discuss the results of such simulations later on in this article. Now it suffices to say that, in general, except ref 38 for NaCl, they corroborate the validity of the CNT. Here, we also make such a comparison to confirm or not the validity of CNT to describe crystal nucleation rates in this particular SCL.

Turning back to germanium, the object of this study, Bording and Taftø[42] first used the seeding method to study the crystallization of a supercooled germanium melt at zero external pressure at a single temperature, $T = 0.625 T_m$. They found that the critical nucleus radius is approximately 1 nm, but they did not evaluate the resulting nucleation rate. Moreover, the used Tersoff interatomic potential greatly overestimates the equilibrium melting temperature, which precludes a comparison of their results with experimental data. Finally, the temperature dependences of the main crystallization parameters of germanium remain open.

In addition to the Tersoff potential, other potentials have been well parameterized for modeling germanium, namely, the Stillinger−Weber (SW), see ref 43 and references therein, and the MEAM.[44] The SW potential was originally developed for the simulation of silicon[45] and has been widely used since then. It was employed here to study germanium crystallization because it has been widely tested, is computationally efficient and applicable for tetrahedral structures, such as that of germanium crystal. The first SW parameterization for describing germanium properties[46] yielded an equilibrium melting temperature of 2885 K,[47] which by far exceeds the experimental value, $T_m = 1211$ K.[21] Later on,[48] a new SW parameterization was proposed, which correctly reproduces the actual T_m. These SW parameters are used in the current research.

Given the above arguments, the main objectives of this study are (i) to obtain, by atomistic simulation, key properties for describing crystal nucleation in supercooled germanium in a wide range of supercoolings and (ii) to test the ability of the MD model and the CNT in predicting the crystal nucleation rates in this substance. To accomplish this task, we will confront experimental values with theoretically calculated nucleation rates using MD generated parameters, namely, the melting point, the macroscopic densities of liquid and crystal phases, the atomic transport coefficient at the liquid/nucleus interface, and the critical nucleus size.

Here, we describe a study of seeded crystallization of supercooled germanium on a zero isobar via MD simulations with the SW potential. The critical nucleus size was obtained directly by simulation at six temperatures covering a range of 200 K. Then, using the critical sizes, equilibrium melting temperature, the melting enthalpy, the effective atomic transport coefficient at the SCL/critical nucleus interface, and the liquid and crystal densities, we estimate the nucleation rates in the framework of the CNT. Finally, we compare the experimentally determined nucleation rates in supercooled germanium with CNT calculations.

The paper is structured as follows. Section 2 gives a brief introduction to the classical theory of crystal nucleation. Section 3 presents the MD model under investigation and the computing procedure. The Results and Discussions are given in Section 4. Section 5 contains the Summary and Conclusions.

2. CLASSICAL NUCLEATION THEORY

The decay of a metastable system is associated with the formation and further growth of critical nuclei. In a SCL at constant temperature, T, and pressure, p, the stationary nucleation rate, J [s^{-1}·m^{-3}]—the average number of viable

https://dx.doi.org/10.1021/acs.jpcb.0c05480
J. Phys. Chem. B 2020, 124, 7979−7988

crystal nuclei formed per unit time per unit volume—can be established.

According to the CNT, the nucleation rate is given by[49]

$$J = \rho \mathcal{D}_* Z_* \exp(-W_*/k_B T) \quad (1)$$

where ρ [m^{-3}] is the number of atoms per unit volume in the SCL, that is, the inverse of the molecular volume; $\mathcal{D}_*$ [s^{-1}] is the effective transport coefficient across the liquid/nucleus interface, which is determined by the mechanism of atom aggregation to the critical nucleus; Z_* is the dimensionless Zeldovich factor ($\sim 10^{-2}$), which characterizes the curvature of the energy barrier at its top and takes into account the dissolution of a fraction of supercritical nuclei; k_B is the Boltzmann constant; and W_* [J] is the work of formation of a spherical critical nucleus, given by

$$W_* = \frac{16\pi}{3} \cdot \frac{\gamma^3}{\rho_*^2 \cdot \Delta\mu^2} \quad (2)$$

Here, γ [J/m^2] is the interfacial free energy of the critical crystal nucleus/SCL; ρ_* [m^{-3}] is the number of atoms in the critical crystal nucleus per unit volume; $\Delta\mu$ [J] is the difference between the chemical potentials of the crystal phase and the SCL, which is the thermodynamic driving force. In eq 2, γ refers to the surface of tension, chosen as the dividing surface between the two states.[50]

In the case of isobaric supercooling, $\Delta\mu$ can be approximated by a widely used expression that gives an upper bound[51]

$$\Delta\mu = \frac{\Delta h_m \Delta T}{T_m} \quad (3)$$

where $\Delta T = T_m - T$, T_m is the equilibrium melting temperature, and Δh_m is the melting enthalpy. This equation is valid when the difference between the specific heat of the SCL and the isochemical crystal approaches zero.

The required thermodynamic work for nucleation, eq 2, corresponds to a certain number of atoms in the (spherical) critical nucleus, n_*, given by

$$n_* = \frac{32\pi}{3} \cdot \frac{\gamma^3}{\rho_*^2 |\Delta\mu|^3} \quad (4)$$

The Zeldovich factor Z_* is given by

$$Z_* = \left(\frac{W_*/k_B T}{3\pi n_*^2} \right)^{1/2} \quad (5)$$

By combining eqs 2, 4, and 5, one can write eq 1 as

$$J = \rho \mathcal{D}_* \left(\frac{\Delta\mu}{6\pi n_* k_B T} \right)^{1/2} \exp\left(-\frac{n_* \Delta\mu}{2 k_B T} \right) \quad (6)$$

Expression 6—the main equation of the CNT—is used here for theoretical calculations of the nucleation rate using parameters obtained from the simulations.

The theoretical evaluation of the transport coefficient $\mathcal{D}_*$ depends on the choice of the model of the determining process near the surface of the growing crystal nuclei. Associating nucleus growth with the frequency of elementary acts of attachment of atoms to its surface and their departure from the surface to the liquid, the following expression is obtained for $\mathcal{D}_*$[52]

$$\mathcal{D}_* = i_* (k_B T/h) \exp(-E/k_B T) \quad (7)$$

where i_* is the number of atoms on the critical nucleus surface, h is the Planck constant, $k_B T/h$ is the atomic vibration frequency, and $E = E(T)$ is the activation energy for the transition of atoms from the SCL to the crystalline nucleus.

3. MD MODEL AND THE COMPUTATIONAL DETAILS

In this paper, we studied the crystallization kinetics of a supercooled Ge liquid at zero isobar at six temperatures: T = 850, 900, 915, 950, 1000, and 1050 K. It should be noted that all these supercoolings can and have been achieved experimentally for Ge.[1] For all investigated supercoolings, the barostat used kept the system pressure in the interval −1.5 to +1.5 bar. Thus, we worked within a pressure range that covers the atmospheric pressure used in the experimental determinations of nucleation rates. Therefore, the actual value of n_* at p = 1 bar is within the 5% uncertainty of the critical size determination.

3.1. MD Model. We carried out the MD simulations in an NpT ensemble, ensuring the constancy of the number of atoms, N, pressure, p, and the temperature, T, of the system. The atoms were located in a cubic cell with 3D periodic boundary conditions.

The interatomic interaction was given by a three-body SW potential.[45]

$$E = \sum_i \sum_{j<i} \phi_2(r_{ij}) + \sum_i \sum_{j\neq i} \sum_{k>j} \phi_3(r_{ij}, r_{ik}, \Theta_{ijk})$$

$$\phi_2(r_{ij}) = A_{ij}\varepsilon_{ij}\left[B_{ij}\left(\frac{\sigma_{ij}}{r_{ij}}\right)^{p_{ij}} - \left(\frac{\sigma_{ij}}{r_{ij}}\right)^{q_{ij}} \right] \exp\left(\frac{\sigma_{ij}}{r_{ij} - a_{ij}\sigma_{ij}} \right)$$

$$\phi_3(r_{ij}, r_{ik}, \Theta_{ijk}) = \lambda_{ijk}\varepsilon_{ijk}[\cos\Theta_{ijk} - \cos\Theta_{0ijk}]^2 \exp\left(\frac{\gamma_{ij}\sigma_{ij}}{r_{ij} - a_{ij}\sigma_{ij}} \right) \exp\left(\frac{\gamma_{ik}\sigma_{ik}}{r_{ik} - a_{ik}\sigma_{ik}} \right) \quad (8)$$

The SW potential reproduces the tetragonal structure of crystalline germanium, taking into account the two- and three-particle interactions, $\phi_2(r_{ij})$ and $\phi_3(r_{ij}, r_{ik}, \theta_{ijk})$ in eq 8, respectively. The parameters for SW potential were taken from ref 48, viz., ε = 1.58 eV, σ = 2.181 Å, a = 1.8, λ = 21, γ = 1.2, $\cos\Theta_0 = -1/3$, A = 7.049556277, B = 0.6022245584, p = 4, q = 0. This SW parameterization was chosen because it correctly reproduces the value of Ge equilibrium melting temperature at atmospheric pressure.[47,48]

MD calculations were carried out using LAMMPS.[53] The time step of integrating the equations of atom motion was 1 fs. The list of neighboring atoms within a radius of 0.2 nm was updated every 10 fs.

For the studied SW model of germanium, the calculated temperature dependences of the densities of the (diamond cubic) crystal, $d_S(T)$, and liquid, $d_L(T)$, along the zero isobar are shown in Figure 1. The values of d_S and d_L were obtained in the NpT ensemble in a system of N = 8000 atoms according to the following procedure. First, a crystal with an ideal diamond lattice was created at a temperature T = 500 K. After 0.1 ns of equilibration, the $d_S(T)$ was averaged over 100 values

https://dx.doi.org/10.1021/acs.jpcb.0c05480
J. Phys. Chem. B 2020, 124, 7979−7988

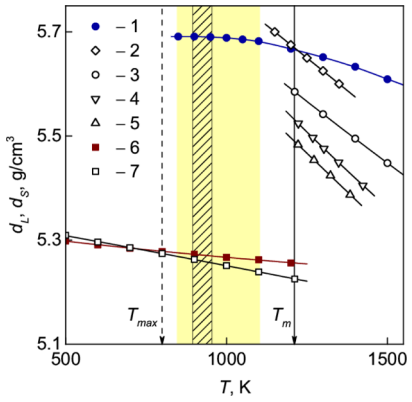

Figure 1. Temperature dependence of the liquid and crystal density of germanium along the zero isobar: current MD calculation of d_L (1) and d_S (6), experimental data on d_L [(2)—ref 55, (3)—ref 7, (4)—ref 8, (5)—ref 54] and d_S [(7)—ref 7]. The experimental values of the melting temperature, T_m = 1211 K,[21] and the temperature of maximum nucleation rate, T_{max} = 800 K,[1] are indicated by vertical lines. The size of the MD symbols corresponds to the determination error. The temperature range of this seeded crystallization MD study is shown in yellow. The temperature range of experimental study of droplet crystallization from refs 1 and 15 is shown by the dashed region.

during the following 0.1 ns. Then, the crystal was heated with a rate of 10^{10} K/s, and again, after equilibration, $d_S(T)$ was calculated. The last studied thermodynamic state of the crystal was at T = 1200 K. Then, the crystal was completely melted by heating to T = 2000 K. After that, similarly, with a cooling step of 100 K, the value of the liquid density, d_L, was calculated in the temperature range T = 800−2000 K. As a phase transformation occurs during the simulation process, it was difficult to calculate $d_L(T)$ below T = 800 K with the cooling rate used.

The calculated MD values of $d_S(T)$ and $d_L(T)$ are in good agreement with the corresponding experimental data, obtained by different experimental techniques[7,8,54−57] and the differences do not exceed 3% at $T = T_m$. Note that the metastable continuation of the experimental $d_L(T)$ coincides with the MD values in the seeded crystallization temperature range (yellow region in Figure 1).

3.2. Melting Point. Determination of the equilibrium melting temperature, T_m, is the starting point in studying liquid supercooling. The value of T_m at zero isobar was determined here by MD simulation using the method of equilibrium coexistence of a crystal and a liquid phase in the NpT ensemble.[58,59] The system creation and equilibration procedures used are described in detail in ref 59. The two-phase system contained N = 25,500 atoms. The crystalline phase was located with the (100) orientation to the flat interface. The densities of the homogeneous phases are independently preliminarily calculated in each thermodynamic state (T,p = 0) under study. The establishment of mechanical equilibrium was verified by the equality of the components of the stress tensor and the hydrostatic pressure of the liquid. From the evolution of the atomic configurations over 10 ns, we found that the two-phase system always crystallized at temperatures T < 1210 K and melted at T > 1230 K (Figure 2). Therefore, the equilibrium temperature is considered T_m = 1220(10) K. The number between brackets indicates the uncertainty in the last significant digits. This value of T_m is in excellent agreement both with a previous estimate, T_m = 1230(50) K,[48] and the

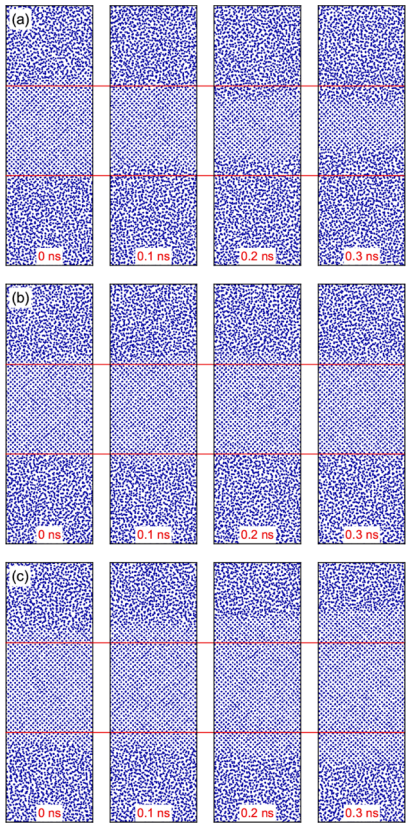

Figure 2. Snapshots (a 155 Å × 65 Å layer of 10 Å thickness) at different times of the solid/liquid system with a flat interface at three temperatures: (a) T = 1270 K, melting; (b) T = 1220 K, equilibrium state; (c) T = 1170 K, crystallization. The total number of atoms is 25,500; approximately 4500 atoms are shown. The horizontal lines are drawn to guide the eyes.

experimental value T_m = 1211 K.[21] Thus, we proceeded with the study of seeded crystallization of liquid germanium in the supercooling range of T/T_m = 0.70−0.86.

The enthalpy of the crystal and liquid phases was determined at T_m = 1211 K and p = 0. Their difference gives the melting enthalpy, $\Delta h_m = 3.77 \times 10^{-20}$ J = 0.235 eV/atom, which is required for the calculation of the thermodynamic driving force, $\Delta\mu$, eq 3. However, this MD value of Δh_m is lower than the experimental value, Δh_m = 0.35 eV/atom.[9] Therefore, in this study, we use these different values to calculate $\Delta\mu$.

3.3. Seeding Parameters. The SCL used for seeded crystallization contained N = 15,000 atoms and was obtained by isobaric cooling from a stable state, T = 1300 K, with a rate of $\Delta T/\Delta t = 10^{10}$ K/s by equilibrating during 0.1 ns. At the geometrical center of the liquid, spheres of variable radii up to 2.0 nm were selected. Then, the atoms inside the spheres were removed, and the space was filled with a fragment of a (perfect diamond cubic) crystal with a lattice constant of 5.678 Å, corresponding to a density of 5.27 g/cm^3.

To prevent atomic overlapping, the inserted spherical crystals always had a radius of 0.05 Å smaller than the radius of the empty region. At each studied temperature, we have embedded crystal nuclei of different dimensions to determine the critical size. Each simulation run only had a single seed in the SCL. Hundreds of independent configurations of SCLs containing a cluster of the same size were studied for reliable statistics. The atomic interaction was described by the SW

https://dx.doi.org/10.1021/acs.jpcb.0c05480
J. Phys. Chem. B 2020, 124, 7979−7988

potential with the same parameterization. The temperature of the crystal seeds was set to be equal to the temperature of the metastable liquid and controlled by the system thermostat.

After equilibrating for 1 ps, the potential energy of the whole system, E_{pot}, was calculated every 5 ps during 1 ns, and the coordinates of all atoms were recorded and analyzed by the q6 order parameter[60,61] to observe the crystal size evolution. The *crystal-like* atoms had at least 11 connected atoms located at the distance of equal or less than 5 Å. The q6 parameter for crystal structure identification was used because of its ability to reveal tetrahedral bonding during SW liquid crystallization.[62]

The properties of the embedded crystalline seed may play a crucial role on the crystallization process. The influence of the seed properties—density, temperature, and structure—on the crystallization kinetics was previously studied by us for a Lennard-Jones liquid crystallization.[33] We concluded that the results of the seeding procedure are indeed sensitive to the starting parameters of the embedded crystalline seed, such as the temperature and structure, but not to their density, at least for small crystalline seeds containing only a few hundred particles. Moreover, for Lennard-Jones liquid, the critical sizes obtained via seeding data are consistent within 10% with their independent estimation by the mean first passage time.[28,33] Therefore, though for the Germanium seeded crystallization a similar investigation has not been carried out so far, we assume that the error of critical size determination does not exceed 10%.

The determination of the exact location of the surface of tension in a computer simulation of seeded/unseeded crystallization is a nontrivial task. In the present study, as in previous similar MD seeding simulations, it is supposed a priori that the radius of the inserted nuclei refers to the surface of tension.

4. RESULTS AND DISCUSSION

A reliable quantitative indicator of the evolution of a crystal seed/SCL system is given by its potential energy, E_{pot}.[33] Therefore, to assess the actual values of the E_{pot} scale, we have calculated the temperature dependences of the potential energies of the crystal and liquid phases, $E_{pot}(T)$, along the zero isobar, which are shown in Figure 3. The computation procedure for E_{pot} was similar to that used for the density calculations.

4.1. Critical Nucleus Size. Figure 4 shows the potential energy evolution of the crystal seed/liquid coexisting phases, $E_{pot}(T)$. During seed growth, that is, during the phase transition, the value of E_{pot} decreases because of the atomic ordering in the metastable liquid caused by crystallization. In the case of complete dissolution of the crystal seed, E_{pot} slightly increased. Note that even after full crystallization, the value of E_{pot} is still larger than that for the ideal crystalline ordering at any given temperature. This is due to the presence of defects in the lattice of the crystalline solid formed during spherical seed growth.

In favorable conditions, critical nuclei could be formed homogeneously in a metastable liquid. However, in this study, during the q6 structure analysis of the whole system, 1 ns, spontaneous formation of supercritical sized nuclei did not occur. In refs 1 and 14 at T = 915 K, the reported experimental homogeneous nucleation rate is $J = 10^{11}$ s^{-1}·m^{-3}. Hence, in the system studied here, viz. N = 15,000 atoms confined in a volume $V \approx 300$ nm^3, the mean waiting time for appearance of the first critical nucleus, $\tau = 1/(J \cdot V)$, would be approximately

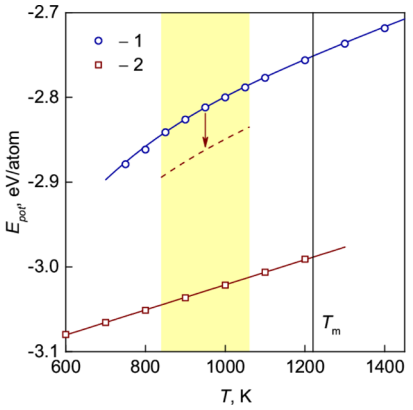

Figure 3. Potential energy per germanium atom, E_{pot}, at p = 0: (1)—liquid phase, (2)—crystal phase. The smooth lines connecting the MD data are an approximation. The temperature range of seeded crystallization study is shown in yellow. The vertical line indicates the equilibrium melting temperature obtained here, T_m = 1220 K. The vertical arrow shows the change in E_{pot} during seeding crystallization studied here; the dashed line shows the values of E_{pot} after 1 ns of crystal growth.

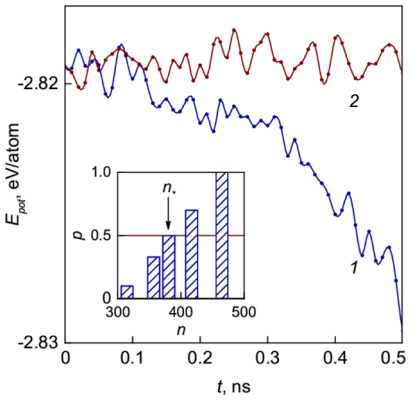

Figure 4. Time dependence of the potential energy of the liquid/crystal seed system, E_{pot}, for two MD seeding simulations at temperature T = 950 K: (1) seed growth; (2) seed decay. E_{pot} are normalized by the total number of atoms in the two-phase system. The zero time refers to the seed insertion into the metastable liquid. Inset: Crystallization probability histogram with nuclei of variable sizes inserted into the SCL at T = 950 K. The horizontal line, p = 0.5, corresponds to a critical size n_* = 380.

one million years. That is why the homogeneous nucleation was not observed in the current research.

With regard to the $E_{pot}(t)$ data (Figure 4), the critical seed sizes—which have an equal probability of growth and dissolution—were determined at each (p, T) state studied. Figure 5 shows the temperature dependence of the number of atoms in the critical crystal seed, $n_*(T)$.

The quantity n_* decreases monotonically from n_* = 1300 to 150 with decreasing temperature as expected from the CNT. The error in the determination of the critical size radius does not exceed 5% and is R_* = 0.94−1.92 nm at T = 850−1050 K, respectively. To a first approximation, R_* is a linear function of the inverse temperature $1/\Delta T$ (inset in Figure 5). Using the seeding method at lower temperatures, T < 850 K, would require small-sized seeds, n < 150, which would lead to large errors associated with incorrectly estimating the number of atoms in the nucleus, because of its numerous surface atoms.[29] Using the seeding method for crystallization at higher

https://dx.doi.org/10.1021/acs.jpcb.0c05480
J. Phys. Chem. B 2020, 124, 7979−7988

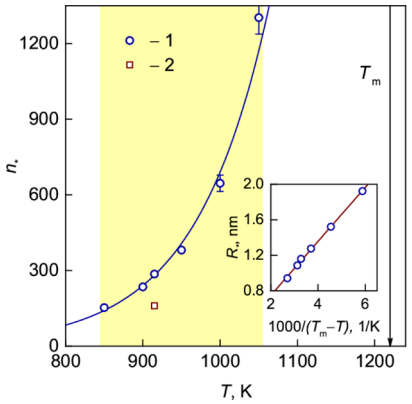

Figure 5. Number of atoms in the critical crystal nucleus, n_*, as a function of temperature at $p = 0$: (1)—current MD calculation by the seeding method, (2)—CNT calculation based on the experimental nucleation rate data of refs 1 and 14. The temperature range of seeded crystallization study is shown in yellow. The vertical line indicates the equilibrium melting temperature, $T_m = 1220$ K. Inset: Radius of the critical nucleus, R_*, as a function of $1/\Delta T$.

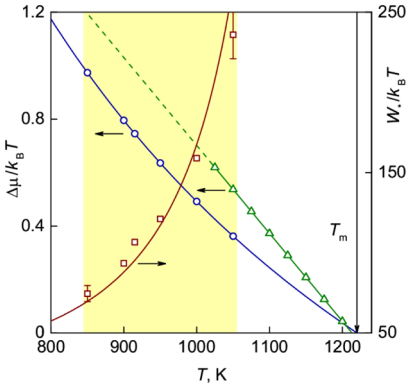

Figure 6. Temperature dependence of the thermodynamic driving force, $\Delta\mu/k_BT$: circles—calculated by eq 3 from this study; triangles—experimental data from ref 9, the dashed line is the linear extrapolation into the deeply supercooled region. Squares—work of critical nucleus formation, $W_*/k_BT = n_*\Delta\mu/2k_BT$, vs temperature, where n_* resulted from our seeding procedure and $\Delta\mu$ was calculated by eq 3. The smooth line, passing through the squares, is the CNT calculation of $W_*(T)$ by eqs 2 and 3 using a constant value of $\gamma = 0.23$ J/m^2. The temperature range of this seeded crystallization study is shown in yellow. The vertical line indicates the equilibrium melting temperature, $T_m = 1220$ K.

temperatures, $T > 1050$ K, is associated with a significant increase in the critical size, that is, the entire system size, which is limited by our computer facilities.

Bording and Taftø have estimated the critical radius, $R_* = 1$ nm, at $T = 0.625T_m$.[42] The exponential extrapolation of $n_*(T)$ in Figure 5 to $T = 0.625T_m \approx 760$ K leads to $n_* = 50$ or $R_*=(3n_*/4\pi\rho_*)^{1/3} = 0.65$ nm. This small disagreement can be explained by using different types of interatomic potentials, that is, Tersoff versus SW.

An indirect estimate of the critical size using experimental nucleation rate data and eq 3 for $\Delta\mu$, yields $n_* = 160$ at $T = 915$ K.[1,14] Our result from the seeding simulation, $n_* = 286$, exceeds somewhat their estimate but is of the same order. In the present simulations, the critical size of $n_* = 160$ corresponds to $T \approx 850$ K.

The stable phase of the germanium crystal has the diamond structure. Therefore, there are eight atoms in the unit cell. Smoothly extrapolating $n_*(T)$ to deeper supercoolings leads to $n_* = 8$ at $T = 0.5T_m \approx 600$ K. As a critical nucleus cannot be smaller than a single unit cell, the CNT is no longer valid below this temperature. However, in this study, we are dealing with shallower supercoolings, $T > 0.7{\cdot}T_m$.

Recently, the influence of the tetrahedral repulsion parameter λ in the SW potential on the thermodynamic properties and phase transitions was established.[63−65] We performed calculations of the effect of λ on seeded crystallization at one temperature. At $T = 915$ K, the critical size $n_* = 286$ was obtained with $\lambda = 21$. We varied λ from 15 to 27 by 1 for interactions of 286 crystal seed atoms; whilst for the interatomic interactions in the SCL, we used a fixed $\lambda = 21$. Ten seed insertion events were carried out for each λ. We found a very strong sensitivity of seeded crystallization to the λ parameter. Namely, at $\lambda \leq 20$, all embedded crystals were dissolved, whereas at $\lambda \geq 22$, they all grew and crystallized the entire system. Therefore, obtaining the $n_*(T,\lambda)$ dependence during crystallization is of fundamental interest and motivates further simulations.

4.2. Thermodynamic Driving Force. The difference between the liquid and solid chemical potentials $\Delta\mu$ was estimated by eq 3. We calculated the thermodynamic driving force (Figure 6) using the MD data—$T_m = 1220$ K and $\Delta h_m = 0.235$ eV/atom. The value of $\Delta\mu$ changes from $0.36{\cdot}k_BT$ at $T = 0.86{\cdot}T_m$ to $0.97{\cdot}k_BT$ at $T = 0.70{\cdot}T_m$. Note that the actual value of $\Delta\mu$ differs from that calculated by eq 3 by up to 20% for the supercooling of $0.7{\cdot}T_m$.[33] On the other hand, in ref 9 the temperature dependence of $\Delta\mu$, down to $T = 0.84{\cdot}T_m$, was thermodynamically calculated from measured data of the heat of melting and specific heat of undercooled Ge melt. Their results on $\Delta\mu(T)$ are higher than our estimate by eq 3 because the experimental value of $\Delta h_m = 465(2)$ J/g[9] exceeds the value resulting from our MD simulations.

4.3. Interfacial Free Energy and the Work of Critical Nucleus Formation. Using the MD data for $n_*(T)$, $\rho_*(T) = \rho_S(T)$, and $\Delta\mu(T)$, calculated by eq 3, the critical nucleus/liquid interfacial free energy was obtained by eq 4. In the studied temperature interval, it is almost constant and equal to $\gamma = 0.23(1)$ J/m^2. Thus, the temperature dependence of $\gamma(T)$, predicted theoretically[66,67] and reliably obtained in a MD simulation of a Lennard-Jones liquid crystallization,[33,68,69] is not revealed for this material in this particular study. However, the obtained value of interfacial free energy, $\gamma = 0.23(1)$ J/m^2, is in excellent agreement with the value calculated here by CNT (where we considered γ as "free" fitting parameter) using experimental data on the crystallization kinetics of supercooled germanium liquid, $\gamma = 0.241$ J/m^2 at $T = 915$ K,[1,14] and with $\gamma = 0.246$ J/m^2 from ref 26, estimated by the Turnbull relation.[27]

Combining eqs 2−4, the work of critical nucleus formation can be obtained: $W_* = n_*\Delta h_m\Delta T/2T_m$. Using the MD data for n_*, Δh_m, T, and T_m, the calculated (reduced) value of the activation barrier W_*/k_BT varies from 74(5) at $T = 0.70{\cdot}T_m$ to 236(15) at $T = 0.86{\cdot}T_m$ (Figure 6). Note that using the experimental values of $\Delta\mu(T)$, linearly extrapolated down to $T = 0.70{\cdot}T_m$, according to eq 2 $W_*\sim 1/\Delta\mu^2$, yields $W_*/k_BT = 49$−107 in the supercooling region under study. As expected, these ranges of W_*/k_BT exceed the values observed in typical brute-force MD studies of crystallization.[4] For example, in the case of homogeneous crystallization of a Lennard-Jones liquid, $W_*/k_BT = 11$−22.[28]

https://dx.doi.org/10.1021/acs.jpcb.0c05480
J. Phys. Chem. B 2020, 124, 7979−7988

The smooth line in Figure 6 shows the CNT calculation of $W_*(T)$ by eqs 2 and 3 using the constant value of $\gamma = 0.23$ J/m^2. The obtained data $W_*(T)$ allows us to estimate the temperature where $W_*/k_BT \approx 1$, that is, where CNT would no longer be valid for this particular MD model of germanium. This temperature, $T = 550(50)$ K, was evaluated by smooth extrapolations of $W_*(T)$.

We also calculated the Zeldovich factor, Z_*, using the data for W_* and n_* in eq 5. The value Z_* takes adequate values and increases from 0.004 at $T = 1050$ K to 0.018 at $T = 850$ K. The use of the experimental values of $\Delta\mu(T)$, linearly extrapolated down to $T = 0.70 \cdot T_m$, leads to a slight change in $Z_* = 0.003-0.015$.

4.4. Transport Coefficient. Finally, to test the validity of CNT, the transport coefficient at the liquid/nucleus interface, $\mathcal{D}_*$, is also needed. Following ref 70, $\mathcal{D}_*$ was obtained from the MD simulations by

$$\mathcal{D}_* = \frac{1}{2}\frac{\langle \Delta n^2(t)\rangle}{t} \tag{9}$$

where $\Delta n(t) = n(t) - n_*$ is the change in the number of atoms in the crystal seed over time. This is the effective attachment coefficient for crystalline nucleus growth. During 0.1 ns after the implementation, every 5 ps, the size of the nucleus $n(t)$ was calculated by analyzing the atom configurations using the q6 method.[60,61] We carried out 50 independent evolutions of the embedded critical crystal $n(t)$ in six thermodynamic states. The slope of the time dependence of $\langle[n(t) - n_*]^2\rangle$ at each temperature determined the value of $\mathcal{D}_*$. The result from the seeded simulations is that $\mathcal{D}_*$ decreases with supercoolings (as expected) and changes by 1 order of magnitude, $\mathcal{D}_* = 10^{12}$ to 10^{13} s^{-1}, in the temperature range $T = 850-1050$ K. The current range of $\mathcal{D}_*$ is consistent with the typical values observed in MD simulations of crystallization of other simple liquids at similar supercoolings.[33,36,68]

Using the MD data for $\mathcal{D}_*$ and n_* in eq 7, the activation energy $E(T)$ was estimated. For this purpose, the number of surface atoms i_* in eq 7 was calculated separately for each inserted seed.[33] In the temperature range investigated, $E = 5.5(2)\ k_BT$. Thus, for supercooled germanium liquid at $T=(0.70-0.86)T_m$, there is a significant superiority of the thermodynamic barrier over the kinetic, that is, $W_*(T) > E(T)$.

Using the values of ρ, $\mathcal{D}_*$, and Z_*, we also calculated the kinetic factor $\rho\mathcal{D}_*Z_*$ in eq 1. This quantity only slightly changes with temperature and is equal to $\rho\mathcal{D}_*Z_* \approx 10^{40}$ s$^{-1}\cdot$m^{-3}. This value is close to that calculated from the CNT based on experimental data of the crystallization of metallic melts, $\rho\mathcal{D}_*Z_* = 10^{38(1)}$ s$^{-1}\cdot$m^{-3}.[1]

4.5. Nucleation Rates. Figure 7 shows the temperature dependence of the calculated and experimental nucleation rate, J, in supercooled germanium liquid at $p = 0$. The theoretical values of J were obtained by eqs 3 and 6 using the MD results for T_m, T, ρ, Δh_m, n_*, and $\mathcal{D}_*$. For the thermodynamic states under investigation, $T = 850-1050$ K, the calculated CNT value of J varies from 10^7 to 10^{-63} s$^{-1}\cdot$m^{-3}. Such a huge change in the magnitude of the nucleation rate with temperature was previously observed in MD simulations of seeded crystallization of methane hydrate,[71] sodium chloride, water, hard spheres, and Lennard-Jones materials.[29] Summarizing, the nucleation rates and other calculated crystallization parameters are shown in Table 1 for all temperatures under investigation.

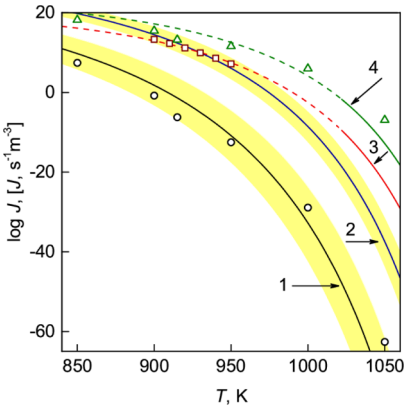

Figure 7. Temperature dependence of the steady-state nucleation rate, $J(T)$: The circles were obtained by eqs 3 and 6 using the MD data for T_m, T, ρ, Δh_m, n_*, and $\mathcal{D}_*$; CNT calculations by eq 10, with the use of eq 3 for $\Delta\mu$, the kinetic factor $\rho\mathcal{D}_*Z_* = 10^{40}$ s$^{-1}\cdot$m^{-3}, and two values of the interfacial free energy: line #1 refers to $\gamma = 0.23(1)$ J/m^2, line #2 refers to $\gamma = 0.201(5)$ J/m^2. The estimated uncertainty of J in γ is shown in yellow. The squares refer to experimental data,[1,15] CNT calculation by eq 10 with $\rho\mathcal{D}_*Z_* = 10^{40}$ s$^{-1}\cdot$m^{-3}, the experimental data of $\Delta\mu(T)$ from ref 9, and two values of the interfacial free energy: line #3 refers to $\gamma = 0.244$ J/m^2, line #4 refers to $\gamma = 0.23$ J/m^2. The dashed continuations of lines #3 and #4 correspond to a linear extrapolation of the experimental $\Delta\mu(T)$ into the deeply supercooled region (Figure 6). The triangles refer to CNT calculation by eq 6 without any fitted parameters using the MD values of $\rho\mathcal{D}_*Z_*$, n_*, and the experimental data for $\Delta\mu(T)$ from ref 9.

The experimental values of the nucleation rate were obtained via multiple measurements of the crystallization waiting times in supercooled germanium droplets of 100−500 μm in diameter.[15] In the temperature range $T \approx 900-950$ K, the value of J changed from approximately 10^8 to 10^{13} s$^{-1}\cdot$m^{-3}. Thus, these experimental values of J exceed by 10−20 o.m. the CNT values estimated here based on MD data using the calculated values of $\Delta\mu(T)$ and Δh_m from the simulations. This discrepancy between the theoretical and experimental values of J is likely a consequence that a huge uncertainty results from using the calculated values of $\Delta\mu(T)$. Also, the crystallization kinetics in this particular (seeded) MD model of germanium is not completely related to experimental observations because the MD results were obtained for an absolutely pure Ge, whereas the real Ge samples used in the experiments have impurities, which might affect somewhat the nucleation rates.

As mentioned above, eq 3 gives an upper bound for the driving force, $\Delta\mu$. However, the experimental values of $\Delta\mu(T)$ are even higher. Therefore, the nucleation rates were recalculated by eq 6 using the experimental values of $\Delta\mu(T)$,[9] linearly extrapolated down to $T = 0.7 \cdot T_m$ (triangles in Figure 7). In this case, we found that the theoretical values of J exceed the experimental values only by 1−4 o.m. It should be observed that, at first sight, these differences seem to be large, but they are much smaller than the reported discrepancies of 20−55 o.m. in the analyses of experimental results.[3] It should be stressed that these values of the nucleation rate were calculated here without any fitting parameter; we only used MD data and the (extrapolated) experimental driving force.

Inserting eq 2 into eq 1 one can write

https://dx.doi.org/10.1021/acs.jpcb.0c05480
J. Phys. Chem. B 2020, 124, 7979−7988

Table 1. Crystallization Parameters at $p = 0$

quantity	temperature, K					
	850	900	915	950	1000	1050
T/T_m	0.70	0.74	0.75	0.78	0.82	0.86
n_*	153	235	286	381	646	1303
R_*, nm	0.94	1.09	1.16	1.28	1.52	1.92
$\Delta\mu/k_BT$, eq 3	0.974	0.795	0.746	0.636	0.492	0.362
$\Delta\mu/k_BT$[9]	1.195	1.030	0.981	0.866	0.701	0.537
W_*/k_BT	74.5	93.4	106.7	121.2	158.9	235.8
Z_*	0.018	0.013	0.012	0.009	0.006	0.004
$\mathcal{D}_*$, 10^{12} s^{-1}	7	10	23	27	46	41
J, s$^{-1}\cdot$m^{-3}, eqs 3 and 6	3×10^{7}	2×10^{-1}	6×10^{-7}	3×10^{-13}	10^{-29}	2×10^{-63}
J, s$^{-1}\cdot$m^{-3}, eq 6 & $\Delta\mu/k_BT$ from ref 9	2×10^{18}	3×10^{15}	2×10^{13}	4×10^{11}	10^{6}	10^{-7}
J, s$^{-1}\cdot$m^{-3}, from ref 1	10^{17}	10^{13}	10^{11}	10^{7}		

$$J = \rho\mathcal{D}_*Z_*\exp\left(-\frac{16\pi}{3}\cdot\frac{\gamma^3}{\rho_*^2\cdot\Delta\mu^2\cdot k_BT}\right) \quad (10)$$

Equation 10 is often used to obtain γ as a fitting parameter in CNT analysis of the experimental values of $J(T)$.

Using the kinetic factor, $\rho\mathcal{D}_*Z_* = 10^{40}$ s$^{-1}\cdot$m^{-3}, the constant value of ρ_*, corresponding to the crystal density of $d_S = 5.27$ g/cm^3,[72] and $\Delta\mu$ from eq 3, the fitted interfacial free energy, $\gamma = 0.23$ J/m^2, we plotted the nucleation rate curve, eq 10, in the studied range of supercoolings (line #1 in Figure 7). The estimated error of J due to the uncertainty in $\gamma = 0.23(1)$ J/m^2 is also shown. The resulting $J(T)$ has the expected dome shape with a maximum at $T \approx 400$ K, which corresponds to $J = 10^{27}$ s$^{-1}\cdot$m^{-3}. However, as the height of the thermodynamic barrier, $W_*(T)$, becomes $\approx 1\cdot k_BT$ at $T = 550$ K and the critical size reaches its limit, $n_* = 8$, at $T = 600$ K, the CNT is no longer valid for this SW Ge liquid at such deep supercoolings. The experimental curve of temperature dependence of the nucleation rate also has a dome shape, with a maximum position at $T \approx 800$ K and $J \approx 10^{18}$ s$^{-1}\cdot$m^{-3}.[1] Thus, the CNT calculation of $J(T)$ based on MD data cannot accurately predict the experimental data $J(T)$. However, the best fitting of the experimental nucleation rates to the theoretical $J(T)$ curve from eq 10 can be achieved with constant values of $\rho\mathcal{D}_*Z_* = 10^{40}$ s$^{-1}\cdot$m^{-3} and γ, used as a "free" parameter: $\gamma = 0.201(5)$ J/m^2 if $\Delta\mu$ is calculated by eq 3 (line #2 in Figure 7) and $\gamma = 0.244$ J/m^2 if the experimental data of $\Delta\mu(T)$ from ref 9 are used (line #3 in Figure 7).

The assumption of no difference between the solid and liquid molar heat capacities, used to evaluate eq 3, results to the linear temperature dependence of the crystal/liquid interfacial free energy, $\gamma(T) = \gamma(T_m)\cdot T/T_m$.[67] CNT describes well the experimental $J(T)$ in a such narrow temperature range, $(0.74-0.78)\cdot T/T_m$, using a constant value of γ (lines #2 and #3 in Figure 7). However, the values of $\gamma(T_m)$ for the real and model germanium have not yet been obtained. Therefore, the question of the temperature dependence of the crystal/liquid interfacial free energy for germanium remains open and motivates further research.

Summarizing, the present analysis corroborates recent studies on seeded crystallization of water, Ni, and NaCl.[35−41] In these papers, the nucleation rate was calculated by eq 6 using eq 9 to obtain the transport coefficient at the liquid/nucleus interface. The thermodynamic driving force was determined by thermodynamic integration, that is, without applying the approximation, eq 3. All these works have shown that the nucleation rates calculated by CNT agree within the error limits, with the experimental values. On the other hand, large discrepancies—from 15 to 30 orders of magnitude—were observed in ref 38 for NaCl crystallization from an aqueous solution. However, later, in ref 40 by the same group, they found the reason for such discrepancies was the inaccuracy in calculating the driving force. The use of revised values of $\Delta\mu$ eliminated such a disagreement.

Thus, our results for Ge crystallization and all the above described studies on seeded crystallization validate the CNT as a good descriptor of the crystal nucleation rates in SCLs, corroborating our recent results of (both seeded and unseeded) MD simulation of supercooled Lennard-Jones and unseeded spontaneous homogeneous nucleation in BaS and NiTi liquids.[33,73,74]

In summary, this is the first systematic MD study on germanium crystallization using a realistic interatomic potential. The SW potential was able to reproduce the density, melting point, and crystal structure. Moreover, to the best of our knowledge, this is the first study that compares simulated nucleation rates with (scarce) experimental values. Finally, it is one of the very few studies that do not use any adjustable parameter in the CNT calculations.

It should be noted that in previous studies of Ge crystallization, for example, in the well-known paper by Bording and Taftø,[42] the chosen Tersoff potential yielded a melting temperature, T_m, that was almost twice higher than the actual melting point of this substance. Therefore, we moved a significant step forward in understanding Ge crystallization in this study, with a T_m that is only 10 K off the experimental value.

However, the interatomic potential used did not yield a reasonable value of the MD—$\Delta\mu$. The experimental values of the driving force are higher than the upper bound, resulting from our Germanium model. Therefore, we recalculated the nucleation rates by eq 6 using the experimental values of $\Delta\mu$ (all other physical quantities were directly derived from the MD simulations). In this case, the theoretical values of J exceed the experimental values only by 1−4 o.m, which is much better that the 20−55 o.m. discrepancy reported for experimental tests of the CNT with glass-forming substances.[3] Most importantly, theoretical nucleation rates were calculated without any fitting parameter; here, we only used MD data and the experimental driving force.

https://dx.doi.org/10.1021/acs.jpcb.0c05480
J. Phys. Chem. B 2020, 124, 7979−7988

5. SUMMARY AND CONCLUSIONS

We carried out comprehensive MD simulations of the crystallization kinetics of a fast quenched germanium liquid at zero pressure, at supercoolings of $0.70{\cdot}T_m$ to $0.86{\cdot}T_m$. We used the seeding method to determine the number of atoms in the critical crystal nuclei at each supercooling, which correspond to spherical radii of $R_* = (1-2)$ nm. The atomic transport coefficient at the SCL/critical crystal nucleus interface, melting point, and melting enthalpy were also obtained by MD.

Combining these quantities directly obtained from the simulations with experimental values of thermodynamic driving force, the calculated values of nucleation rates are only a few orders of magnitude higher than the experimental values, whereas using the calculated values of $\Delta\mu(T)$, the calculated nucleation rates are below the experimental values. Therefore, without using any fit parameter, the calculated nucleation rates using the experimental and calculated values of $\Delta\mu(T)$ embrace the experimental $J(T)$ curve. This study for Ge corroborates previous results for seeded crystallization of Lennard-Jones liquid, H_2O, NaCl, and Ni and favors the validity of the CNT for simple, double, and monoatomic substances.

AUTHOR INFORMATION

Corresponding Author

Azat O. Tipeev − *Department of Physics, Federal University of São Carlos, 13565-905 São Carlos, São Paulo, Brazil;* orcid.org/0000-0002-6939-7339; Email: azattipeev@gmail.com

Authors

Edgar D. Zanotto − *Department of Materials Engineering, Federal University of São Carlos, 13565-905 São Carlos, São Paulo, Brazil;* orcid.org/0000-0003-4931-4505

José P. Rino − *Department of Physics, Federal University of São Carlos, 13565-905 São Carlos, São Paulo, Brazil*

Complete contact information is available at: https://pubs.acs.org/10.1021/acs.jpcb.0c05480

Notes

The authors declare no competing financial interest.

The data that support the findings of this study are available from the corresponding author upon reasonable request.

ACKNOWLEDGMENTS

A.O.T. acknowledges the São Paulo Research Foundation (FAPESP) for his postdoctoral fellowship (Grant 2017/08350-1). E.D.Z. and J.P.R. also thank FAPESP (contract CEPID 2013/07793-6) for the financial support of this research. Finally, we appreciate the critical comments of Alexander Abyzov, Vladimir Fokin, and Jincheng Du. All MD results were obtained using the computer facilities of the Physics Department, Federal University of São Carlos, Brazil.

REFERENCES

(1) Skripov, V. P.; Koverda, V. P. *Spontaneous Crystallization of Supercooled Liquids*; Nauka: Moscow, 1984.

(2) Kelton, K. F.; Greer, A. L. *Nucleation in Condensed Matter: Applications in Materials and Biology*, 1st ed.; Pergamon: U.K., 2010.

(3) Fokin, V. M.; Zanotto, E. D.; Yuritsyn, N. S.; Schmelzer, J. W. P. Homogeneous crystal nucleation in silicate glasses: a 40 years perspective. *J. Non-Cryst. Solids* **2006**, *352*, 2681−2714.

(4) Sosso, G. C.; Chen, J.; Cox, S. J.; Fitzner, M.; Pedevilla, P.; Zen, A.; Michaelides, A. Crystal nucleation in liquids: open questions and future challenges in molecular dynamics simulations. *Chem. Rev.* **2016**, *116*, 7078−7116.

(5) Yonenaga, I. Germanium crystals. In *Single Crystals of Electronic Materials: growth and properties*; Fornari, R., Ed.; Woodhead Publishing, 2019; pp 89−127.

(6) *Germanium-Based Technologies: from Materials to Devices*; Claeys, C., Simoen, E., Eds.; Elsevier, 2007.

(7) Stankus, S. V.; Khairulin, R. A.; Tyagel'skii, P. V. The thermal properties of germanium and silicon in condensed state. *High Temp.* **1999**, *37*, 559−564.

(8) Glazov, V. M.; Shchelikov, O. D. Volume changes during melting and heating of silicon and germanium melts. *High Temp.* **2000**, *38*, 405−412.

(9) Li, Q.; Zhu, Y. Y.; Liu, R. P.; Li, G.; Ma, M. Z.; Yu, J. K.; He, J. L.; Tian, Y. J.; Wang, W. K. Specific heat and related thermodynamic properties of an undercooled germanium melt. *Appl. Phys. Lett.* **2004**, *85*, 558−560.

(10) Turnbull, D.; Cech, R. E. Microscopic observation of the solidification of small metal droplets. *J. Appl. Phys.* **1950**, *21*, 804−810.

(11) Fehling, J.; Scheil, E. Supercooling of molten metals. *Z. Metallkd* **1962**, *53*, 593−600.

(12) Powell, G. L. F. Undercooling of germanium. *Trans. Metall. Soc. AIME* **1967**, *239*, 1662−1663.

(13) Li, D. L.; Volkmann, T.; Eckler, K.; Herlach, D. M. Crystal growth in undercooled germanium. *J. Cryst. Growth* **1995**, *152*, 101−104.

(14) Skripov, V. P.; Koverda, V. P.; Butorin, G. T. Kinetics of crystal nucleation in small volumes. *Crystal Growth*; University of Yerevan, 1975; Vol. *11*, pp 25−29.

(15) Koverda, V. P.; Skripov, V. P. Spontaneous crystallization of supercooled liquid metals. *Phys. Met. Metallogr.* **1973**, *35*, 988−992.

(16) Devaud, G.; Turnbull, D. Undercooling of molten silicon. *Appl. Phys. Lett.* **1985**, *46*, 844−845.

(17) Devaud, G.; Turnbull, D. Microstructures of undercooled Germanium droplets. *Acta Metall.* **1987**, *35*, 765−769.

(18) Li, D.; Eckler, K.; Herlach, D. M. Development of grain structures in highly undercooled germanium and copper. *J. Cryst. Growth* **1996**, *160*, 59−65.

(19) Li, D.; Eckler, K.; Herlach, D. M. Undercooling, crystal growth and grain structure of levitation melted pure Ge and Ge-Sn alloys. *Acta Mater.* **1996**, *44*, 2437−2443.

(20) Filipponi, A.; Malvestuto, M. An experimental set-up for the nucleation rate determination in supported undercooled liquid metal droplets. *Meas. Sci. Technol.* **2003**, *14*, 875−882.

(21) *CRC Handbook of Chemistry and Physics*, 87th ed.; Lide, D. R., Ed.; CRC Press, Boca Raton, 2006.

(22) Barna, Á.; Barna, P. B.; Pócza, J. F. Crystallization processes in a-Ge thin films. *J. Non-Cryst. Solids* **1972**, *8−10*, 36−44.

(23) Blum, N. A.; Feldman, C. The crystallization of amorphous germanium films. *J. Non-Cryst. Solids* **1976**, *22*, 29−35.

(24) Germain, P.; Zellama, K.; Squelard, S.; Bourgoin, J. C.; Gheorghiu, A. Crystallization in amorphous germanium. *J. Appl. Phys.* **1979**, *50*, 6986−6994.

(25) Kim, Y.-W.; Lin, H.-M.; Kelly, T. F. Amorphous solidification of pure metals in submicron spheres. *Acta Metall.* **1989**, *37*, 247−255.

(26) Vučí, Z.; Subaší, D.; Ogorelec, Z. The determination of the crystal-liquid interfacial tension in germanium. *Phys. Status Solidi A* **1978**, *47*, 703−710.

(27) Turnbull, D. Formation of crystal nuclei in liquid metals. *J. Appl. Phys.* **1950**, *21*, 1022−1028.

(28) Baidakov, V. G.; Tipeev, A. O. Crystal nucleation and the solid-liquid interfacial free energy. *J. Chem. Phys.* **2012**, *136*, 074510.

(29) Espinosa, J. R.; Vega, C.; Valeriani, C.; Sanz, E. Seeding approach to crystal nucleation. *J. Chem. Phys.* **2016**, *144*, 034501.

(30) Bergfors, T. Seeds to Crystals. *J. Struct. Biol.* **2003**, *142*, 66−76.

(31) Parambil, J. V.; Heng, J. Y. Y. Seeding in Crystallisation. In *Engineering Crystallography: From Molecule to Crystal to Functional Form*; Roberts, K., Docherty, R., Tamura, R., Eds.; Springer: Dordrecht, 2017; pp 235−245.
(32) Uttormark, M. J.; Thompson, M. O.; Clancy, P. Kinetics of crystal dissolution for a Stillinger-Weber model of silicon. *Phys. Rev. B: Condens. Matter Mater. Phys.* **1993**, *47*, 15717−15726.
(33) Tipeev, A. O.; Zanotto, E. D.; Rino, J. P. Diffusivity, interfacial free energy, and crystal nucleation in a supercooled Lennard-Jones liquid. *J. Phys. Chem. C* **2018**, *122*, 28884−28894.
(34) Bai, X.-M.; Li, M. Calculation of solid-liquid interfacial free energy: a classical nucleation theory based approach. *J. Chem. Phys.* **2006**, *124*, 124707.
(35) Sanz, E.; Vega, C.; Espinosa, J. R.; Caballero-Bernal, R.; Abascal, J. L. F.; Valeriani, C. Homogeneous ice nucleation at moderate supercooling from molecular simulation. *J. Am. Chem. Soc.* **2013**, *135*, 15008−15017.
(36) Espinosa, J. R.; Sanz, E.; Valeriani, C.; Vega, C. Homogeneous ice nucleation evaluated for several water models. *J. Chem. Phys.* **2014**, *141*, 18C529.
(37) Espinosa, J. R.; Zaragoza, A.; Rosales-Pelaez, P.; Navarro, C.; Valeriani, C.; Vega, C.; Sanz, E. Interfacial free energy as the key to the pressure-induced deceleration of ice nucleation. *Phys. Rev. Lett.* **2016**, *117*, 135702.
(38) Zimmermann, N. E. R.; Vorselaars, B.; Quigley, D.; Peters, B. Nucleation of NaCl from aqueous solution: critical sizes, ion attachment kinetics, and rates. *J. Am. Chem. Soc.* **2015**, *137*, 13352−13361.
(39) Espinosa, J. R.; Vega, C.; Valeriani, C.; Sanz, E. The crystal-fluid interfacial free energy and nucleation rate of NaCl from different simulation methods. *J. Chem. Phys.* **2015**, *142*, 194709.
(40) Zimmermann, N. E. R.; Vorselaars, B.; Espinosa, J. R.; Quigley, D.; Smith, W. R.; Sanz, E.; Vega, C.; Peters, B. NaCl nucleation from brine in seeded simulations: sources of uncertainty in rate estimates. *J. Chem. Phys.* **2018**, *148*, 222838.
(41) Sun, Y.; Song, H.; Zhang, F.; Yang, L.; Ye, Z.; Mendelev, M. I.; Wang, C.-Z.; Ho, K.-M. Overcoming the time limitation in molecular dynamics simulation of crystal nucleation: a persistent-embryo approach. *Phys. Rev. Lett.* **2018**, *120*, 085703.
(42) Bording, J. K.; Taftø, J. Molecular-dynamics simulation of growth of nanocrystals in an amorphous matrix. *J. Phys. Rev. B* **2000**, *62*, 8098−8103.
(43) Posselt, M.; Gabriel, A. Atomistic simulation of amorphous germanium and its solid phase epitaxial recrystallization. *Phys. Rev. B: Condens. Matter Mater. Phys.* **2009**, *80*, 045202.
(44) Kim, E. H.; Shin, Y.-H.; Lee, B.-J. A modified embedded-atom method interatomic potential for Germanium. *Calphad* **2008**, *32*, 34−42.
(45) Stillinger, F. H.; Weber, T. A. Computer simulation of local order in condensed phases of silicon. *Phys. Rev. B: Condens. Matter Mater. Phys.* **1985**, *31*, 5262−5271.
(46) Ding, K.; Andersen, H. C. Molecular-dynamics simulation of amorphous germanium. *Phys. Rev. B: Condens. Matter Mater. Phys.* **1986**, *34*, 6987−6991.
(47) López, P.; Pelaz, L.; Santos, I.; Marqués, L. A.; Aboy, M. Molecular dynamics simulations of damage production by thermal spikes in Ge. *J. Appl. Phys.* **2012**, *111*, 033519.
(48) Nordlund, K.; Ghaly, M.; Averback, R. S.; Caturla, M.; Diaz de la Rubia, T.; Tarus, J. Defect production in collision cascades in elemental semiconductors and fcc metals. *Phys. Rev. B: Condens. Matter Mater. Phys.* **1998**, *57*, 7556−7570.
(49) Zeldovich, J. B. Contribution to the Theory of the Formation of a New Phase. *J. Exp. Theor. Phys.* **1942**, *12*, 525−538.
(50) Gibbs, J. W. *The Collected Works*; Longmans & Green: New York, London, Toronto, 1928; Vol. *1*.
(51) Kelton, K. F. Crystal nucleation in liquids and glasses. *Solid State Phys.* **1991**, *45*, 75−177.
(52) Turnbull, D.; Cormia, R. L. Kinetics of crystal nucleation in some normal alkane liquids. *J. Chem. Phys.* **1961**, *34*, 820−831.
(53) Plimpton, S. Fast parallel algorithms for short-range molecular dynamics. *J. Comput. Phys.* **1995**, *117*, 1−19.
(54) Gegel, A. R.; Glazov, V. M. *Physical properties of electronic melts*; Nauka: Moscow, 1980.
(55) Rhim, W.-K.; Ishikawa, T. Thermophysical Properties of Molten Germanium Measured by the High Temperature Electrostatic Levitator. *Proceedings of the 5th Asian Thermophysical Properties Conference; Seoul*; National University, 1998; pp 611−616.
(56) Sato, Y.; Nishizuka, T.; Tachikawa, T.; Hoshi, M.; Yamamura, T.; Waseda, Y. Viscosity and density of molten germanium. *High. Temp.−High. Press.* **2000**, *32*, 253−260.
(57) Chathoth, S. M.; Damaschke, B.; Samwer, K.; Schneider, S. Thermophysical properties of Si, Ge, and Si−Ge alloy melts measured under microgravity. *Appl. Phys. Lett.* **2008**, *93*, 071902.
(58) Morris, J. R.; Wang, C. Z.; Ho, K. M.; Chan, C. T. Melting line of aluminum from simulations of coexisting phases. *Phys. Rev. B: Condens. Matter Mater. Phys.* **1994**, *49*, 3109−3115.
(59) Baidakov, V. G.; Protsenko, S. P.; Tipeev, A. O. Temperature dependence of the crystal-liquid interfacial free energy and the endpoint of the melting line. *J. Chem. Phys.* **2013**, *139*, 224703.
(60) ten Wolde, R. P.; Ruiz-Montero, M. J.; Frenkel, D. Numerical calculation of the rate of crystal nucleation in a Lennard-Jones system at moderate undercooling. *J. Chem. Phys.* **1996**, *104*, 9932−9947.
(61) Steinhardt, P. J.; Nelson, D. R.; Ronchetti, M. Bond-orientational order in liquids and glasses. *Phys. Rev. B: Condens. Matter Mater. Phys.* **1983**, *28*, 784−805.
(62) Li, T.; Donadio, D.; Galli, G. Nucleation of tetrahedral solids: a molecular dynamics study of supercooled liquid silicon. *J. Chem. Phys.* **2009**, *131*, 224519.
(63) Molinero, V.; Sastry, S.; Angell, C. A. Tuning of tetrahedrality in a silicon potential yields a series of monatomic (metal-like) glass formers of very high fragility. *Phys. Rev. Lett.* **2006**, *97*, 075701.
(64) Bhat, M. H.; Molinero, V.; Soignard, E.; Solomon, V. C.; Sastry, S.; Yarger, J. L.; Angell, C. A. Vitrification of a monatomic metallic liquid. *Nature* **2007**, *448*, 787−790.
(65) Fijan, D.; Wilson, M. Liquid state anomalies and the relationship to the crystalline phase diagram. *Phys. Rev. E* **2019**, *99*, 010103.
(66) Schmelzer, J. W. P.; Abyzov, A. S. Crystallization of glass-forming liquids: thermodynamic driving force. *J. Non-Cryst. Solids* **2016**, *449*, 41−49.
(67) Schmelzer, J. W. P.; Abyzov, A. S. Crystallization of glass-forming liquids: specific surface energy. *J. Chem. Phys.* **2016**, *145*, 064512.
(68) Baidakov, V. G.; Protsenko, K. R. Spontaneous crystallization of a supercooled Lennard-Jones liquid: molecular dynamics simulation. *J. Phys. Chem. B* **2019**, *123*, 8103−8112.
(69) Montero de Hijes, P.; Espinosa, J. R.; Sanz, E.; Vega, C. Interfacial free energy of a liquid-solid interface: its change with curvature. *J. Chem. Phys.* **2019**, *151*, 144501.
(70) Auer, S.; Frenkel, D. Numerical prediction of absolute crystallization rates in hard-sphere colloids. *J. Chem. Phys.* **2004**, *120*, 3015−3029.
(71) Knott, B. C.; Molinero, V.; Doherty, M. F.; Peters, B. Homogeneous nucleation of methane hydrates: unrealistic under realistic conditions. *J. Am. Chem. Soc.* **2012**, *134*, 19544−19547.
(72) $\rho_* = N_A \cdot d_S/m_0$, where N_A is Avogadro number and m_0 = 72.63 g/mol is the germanium atomic weight.
(73) Prado, S. C. C.; Rino, J. P.; Zanotto, E. D. Successful test of the classical nucleation theory by molecular dynamic simulations of BaS. *Comput. Mater. Sci.* **2019**, *161*, 99−106.
(74) Tipeev, A. O.; Zanotto, E. D. Nucleation kinetics in supercooled Ni50Ti50: Computer simulation data corroborate the validity of the Classical Nucleation Theory. *Chem. Phys. Lett.* **2019**, *735*, 136749.

https://dx.doi.org/10.1021/acs.jpcb.0c05480
J. Phys. Chem. B 2020, 124, 7979−7988